PROCEEDINGS A

rspa.royalsocietypublishing.org

Research

Article submitted to journal

**Subject Areas:**
structural engineering, mechanical engineering, mechanics

**Keywords:**
reconfigurable origami, mechanics of origami tubes, variable cross-section tubes, programmable structures

**Author for correspondence:**
G. H. Paulino
e-mail: paulino@gatech.edu

# Origami tubes with reconfigurable polygonal cross-sections

E. T. Filipov[1], G. H. Paulino[1,2] and T. Tachi[3]

[1]Department of Civil and Environmental Engineering, University of Illinois at Urbana-Champaign, Urbana, Illinois 61801, USA
[2]School of Civil and Environmental Engineering, Georgia Institute of Technology, Atlanta, Georgia 30332, USA
[3]Department of General System Studies, University of Tokyo, 3-8-1 Komaba, Meguro-Ku, Tokyo 153-8902, Japan

Thin sheets can be assembled into origami tubes to create a variety of deployable, reconfigurable, and mechanistically unique three dimensional structures. We introduce and explore origami tubes with polygonal, translational symmetric cross-sections, that can reconfigure into numerous geometries. The tubular structures satisfy the mathematical definitions for flat and rigid foldability, meaning that they can fully unfold from a flattened state with deformations occurring only at the fold lines. The tubes do not need to be straight, and can be constructed to follow a non-linear curved line when deployed. *The cross-section and kinematics of the tubular structures can be reprogrammed by changing the direction of folding at some folds.* We discuss the variety of tubular structures that can be conceived and we show limitations that govern the geometric design. We quantify the global stiffness of the origami tubes through eigenvalue and structural analyses and highlight the mechanical characteristics of these systems. The two-scale nature of the present work indicates that, from a local viewpoint, the cross-section of the polygonal tubes are reconfigurable while, from a global viewpoint, deployable tubes of desired shapes are achieved. This class of tubes has potential applications ranging from pipes and micro-robotics to deployable architecture in buildings.



THE ROYAL SOCIETY PUBLISHING

## 1. Introduction

Historically, origami has gained popularity in science and engineering because a compactly stowed or flat system can be folded into a transformable 3D structure with increased functionality. Proposed applications in the smaller length scales include biomedical devices [1], and micro robotic assembly [2]. In medium sizes, origami techniques have been used in creating compliant mechanisms [3], actuators [4], toys, and educational tools [5]. Large origami structures could be constructed for aerospace [6] and architectural applications [7]. The applications seem to be endless.

More recently, innovation with origami has pivoted on its capability to create programmable and re-programmable systems that can change shape, function, and mechanical properties. For example Hawkes et al. [8] created a sheet with pre-defined fold lines that can reshape autonomously into different three dimensional structures. Marras et al. [9] showed that DNA can be folded to create nano-scale mechanisms with programmable mechanical function. Origami metamaterials that can be reconfigured, and whose mechanical properties can be tuned and tailored have also become a popular subject of study [10–13].

Thin walled origami tubes have been created by folding thin sheets, but they typically differ from the fundamental definitions of origami. In particular: entire origami tubes are not *developable*, meaning they cannot be created from a continuous flat sheet; and they require gluing or some other connectivity for creating the complete tube. Despite the higher complexity of manufacturing, origami tubes greatly extend the functionality of engineered thin sheet structures. For example, they can be be used as deployable stents in biomedicine [14], as inflatable structural booms for space structures [15,16], or as actuators and bellows [4,17,18]. Origami tubes have a self-constraining geometry that makes them suitable for energy absorption devices [19–22]. Stacking and coupling of origami tubes into more complex geometries can lead to stiffening of the system and enhanced mechanical characteristics [11,13,23,24].

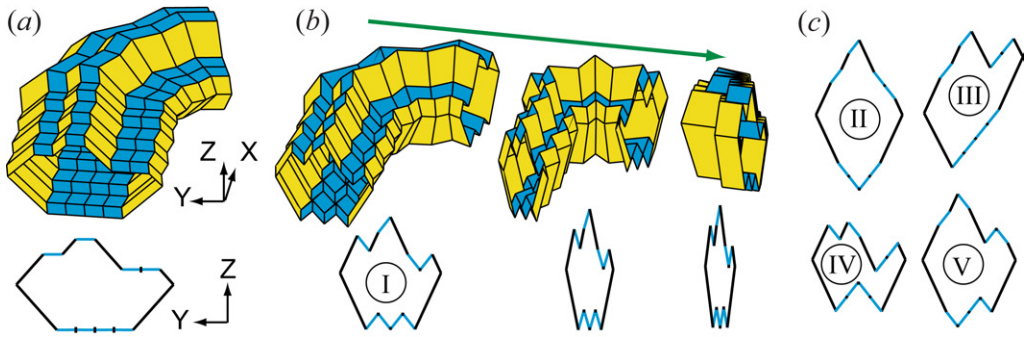


**Figure 1.** A reconfigurable origami tube with a polygonal cross-section. (*a*) The tube and cross-section shown at a fully extended state. (*b*) Folding sequence of the tube, where the cross-section is reconfigured using the four initially flat panels or *switches* ($n = 4$). (*c*) Four other possible cross-sections into which the tube can be reconfigured.

A variety of origami inspired tubes exist including the Miura-Tachi polyhedron [17,25,26], and variations inspired by the Yoshimura pattern [27]. In this paper, we explore and extend upon origami tubes that employ the Miura-ori pattern, that were first introduced by Tachi and Miura [28,29]. We generalize these into a new set of polygonal cross-section tubes that posses the following properties and advantages:

1. Tube cross-sections can take a variety of polygonal shapes.
2. The cross-sections can be made reconfigurable to allow for programmable functionality.
3. A wide variety of new curved tubular forms are possible.

4. The tubes are compatible and can be coupled into a variety of assemblages.
5. The mechanical properties of the tubes can be tuned through reconfiguration.
6. Out-of-plane compression stiffness is enhanced similar to corrugated pipe systems.
7. The perimeter of the tubes is continuous, allowing for deployment by inflation and for the potential capability to carry liquids and gases.
8. Based on idealized zero-thickness kinematics, the tubes are *flat foldable* meaning that they can fold down to a completely flat state allowing for compact stowage.
9. These systems are *rigid foldable*, meaning the origami can fold and unfold with deformation concentrated only along the fold lines (creases), while the panels (facets) remain flat. This capability could allow the structures to be constructed with panels of finite thickness [30–32], and to fold in a controlled motion.

Properties 1, 2, 3, 5, and 6 are possible with the new polygonal tube definitions presented herein. Some of the advantages are motivated by figure 1 that shows a curved tube that can fold in a variety of different cross-sections. The versatility, mechanical characteristics and reconfigurability of theses tubes could result in numerous applications as pipelines, architectural structures, robotic components, bellows, metamaterials, and other reprogrammable systems.

The paper is organized as follows: Section 2 introduces the cross-sections, and Section 3 provides the full three dimensional definition for admissible polygonal tubes. The system kinematics and reconfigurable characteristics of different tubes are discussed in Section 4. In Section 5 we extend the tubular definitions to cellular assemblages that can also be reconfigured. In Section 6 we discuss the elastic modelling and explore the mechanical properties of the tubes through eigenvalue and structural analyses. Tubes with circular cross-sections are investigated in Section 7, and Section 8 provides a discussion and concluding remarks. Appendix A explains folding characteristics of the idealized tubes assuming zero-thickness, Appendix B gives an analytical comparison between smooth pipes and origami tubes, and Appendix C gives an outlook for practical implementations and future extensions of the proposed systems.

## 2. Cross-section definitions for polygonal tubes

The popular Miura-ori pattern has inspired the development of rigid foldable origami tubes discussed in several recent articles [13,23–25,28,29,33]. The cross-sections of these tubes are symmetric, with the most fundamental tube consisting of two equal symmetric Miura-ori strips placed opposite from each other. More advanced cross-sections follow isotropic, anisotropic, or star shaped cylindrical variations [25,28,29]. In this work, we go beyond the previous tube variations and introduce a *translational symmetry method* to create a variety of polygonal shaped tubes. The basic cross-section variations for the polygonal tubes are defined in the $Y-Z$ axis, as demonstrated by figure 2. For our definition, we divide the geometry of the cross-section into an upper ($U$) and a lower ($L$) *section*. The names of these two sections are only representative and their location may in fact be side by side as shown later in figures 3 and 4. The two opposing sections of the tube have to be continuous and can be composed of $m \geq 2$ *edge groups*. The edge groups are identified by a unique slope angle $\theta$, and denoted by a lower-case letter ($a$, $b$, $c$ ...). The slope angle is taken clockwise from the $Z$ axis of the cross-section, and has the admissible range of $-180^\circ < \theta < 180^\circ$. Each edge group on the upper section can be composed of $p \geq 1$ *edges*, and the corresponding lower edge group can be composed of $q \geq 1$ *edges*. The length of the $i^{\text{th}}$ edge in the $b$ edge group on the upper ($U$) section is denoted as $b_{Ui}$.

To create a valid cross-section, each edge group on the upper section must have a corresponding edge group on the lower section with the same total length and slope angle. This definition can be written mathematically as:

$$\sum_{i=1}^{p} a_{Ui} = \sum_{i=1}^{q} a_{Li}; \qquad \sum_{i=1}^{p} b_{Ui} = \sum_{i=1}^{q} b_{Li} \qquad \ldots \qquad \sum_{i=1}^{p} m_{Ui} = \sum_{i=1}^{q} m_{Li}, \tag{2.1}$$

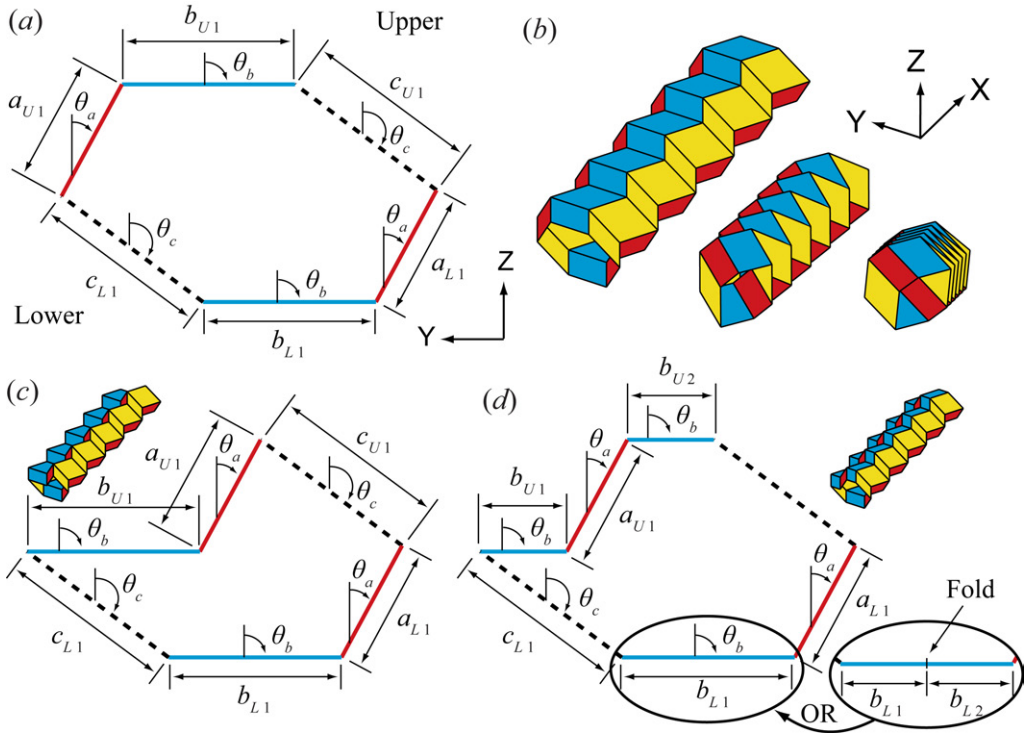


**Figure 2.** Valid cross-section definitions and basic variations. (*a*) Six-sided tube cross-section with $m = 3$ edge groups each having a unique slope angle $\theta$. (*b*) Folding sequence of a tube created from the cross-section in (*a*). The cross-section corresponds to the fully-extended configuration. (*c*) Six-sided cross-section with the same edge groups as in (*a*), arranged in a different order. (*d*) The upper edge group $b_U$ is divided in two ($p = 2$) and rearranged. The corresponding lower edge group $b_L$ can be composed of a single, two, or more corresponding edges with an equal total length ($q \neq p$).

This property ensures that the cross-section will be closed, thus creating a foldable origami tube with a continuous un-interrupted circumference. The logic of equation (2.1) can also be though of as a sum of two groups (sections) of equal direction vectors (edge groups), segmented (into edges) and re-arranged to create the cross-section. The re-arrangement of the individual edges can be performed in any logical manner (e.g. figure 2*c*), so long as the lower and upper sections do not intersect. As shown in figure 2*d*, when an edge group is segmented into several edges, the number of edges on the upper and lower sections do not need to be the same (i.e. $p \neq q$). A non-trivial cross-sections with a negative $\theta$ is shown in figure 3 and one with a complex outline is shown in figure 4.

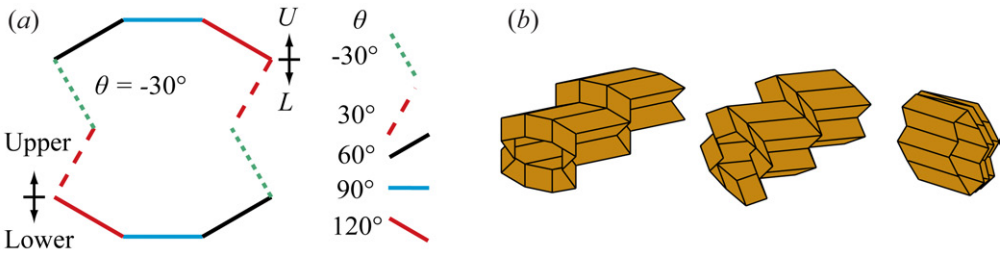


**Figure 3.** (*a*) Cross-section with a negative slope angle $\theta$. (*b*) A tube with that cross-section shown fully extended, and folded to 95% and 10% extension.

The fundamental tube that was previously studied [28,33] is a unique case of the generalization proposed here. The tube is created from only four edges that are symmetric about the $Y$ and $Z$ axes; that is $\theta_B = 180^\circ - \theta_A$, and the edge lengths are $a_{U1} = a_{L1} = b_{U1} = b_{L1}$. This tube can be fully flattened in the $X-Y$ plane and can also be folded into a flat state in the $Y-Z$ plane. However, as will be shown in Section 4, this most fundamental tube case is not reconfigurable. To create a reconfigurable tube, the cross-section must have at least three edge groups ($m > 2$) each with a unique slope angle $\theta$. Although the slope angles can be arbitrary, in our work we define reconfigurable cross-sections with one edge group where $\theta = 90^\circ$. When this cross-section is projected in the $X-Y$ plane per Section 3(a), the $\theta = 90^\circ$ edge group will be completely flat. As defined, the tube is at a fully extended state (100% extension), because from this state the flat edge group can only fold down. When folding, the $\theta = 90^\circ$ edges serve as programmable bits or *switches* to reconfigure the tube cross-section (see Section 4). A $m > 2$ cross-section that has no edge group with $\theta = 90^\circ$, is not fully extended when initially defined, and the edges with $\theta$ closest to $90^\circ$ serve as the switches.

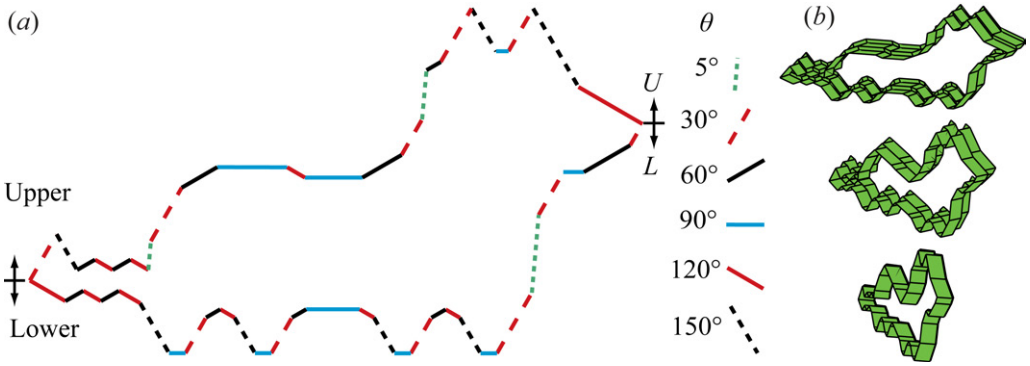


**Figure 4.** (*a*) An admissible cross-section with the shape of a dog, created with six different edge groups. The upper section has 22 edges, while the lower section has 29. (*b*) Dog tube fully extended, and folded to 95% and 10% extension.

## 3. Three dimensional profile definitions

In this section, we discuss the complete three dimensional definition of the tubes when a previously defined $Y-Z$ cross-section is used as a basis. The cross-section is projected in $X-Y-Z$ space, to create a closed continuous tube. The tube definitions assume that the origami sheets have an infinitesimally small or zero-thickness. In practice, there is a technique that allows for thickness to be incorporated into the design of rigid foldable tubes [31], however we do not take these details into account. In Section 3(a) we discuss the basic projection geometries that preserve the rigid and flat foldability of the polygonal origami tubes. *With these definitions the capability to reconfigure the cross-section is preserved allowing for a programmable system.* The projection discussed in Section 3(b) violates flat foldability conditions, but maintains rigid foldability and the programmable characteristics. The projection presented in Section 3(c) is the most geometrically unrestricted, but it restricts folding for non-square, non-symmetric tubes. The programmable characteristics of the tubes are discussed in Section 4, and the folding properties are summarized in Appendix A.

## (a) Admissible projections for rigid and flat foldable polygonal origami tubes

The first geometric variation for the tubes is to project the the cross-section in the $X-Y$ plane with a constant projection angle as shown in figure 5*a-d*. The projection is defined by an angle $\phi$ and length $l$. This projection creates a new cross-section that again lies only in the $Y-Z$ plane and is parallel with the initial cross-section when looked at from above ($X-Y$ plane). The corresponding edges of the two cross-sections are connected with thin origami sheets creating a system of fold lines and panels. A different projection angle $\phi$ can be used to create a distinctly different structure (figure 5*b* and *c*). The length of individual projected segments can also be varied (figure 5*d*). When the base projection with no length variation is used, all panels are parallelograms and are the same for each cross-section edge. The left vertex angle ($\alpha$) of each panel (internal angle of the parallelogram) can be calculated as $\alpha_L = \arccos(-\sin(\theta) * \cos(\phi))$. For other more complex projections discussed herein we leave the geometric derivations to the reader.

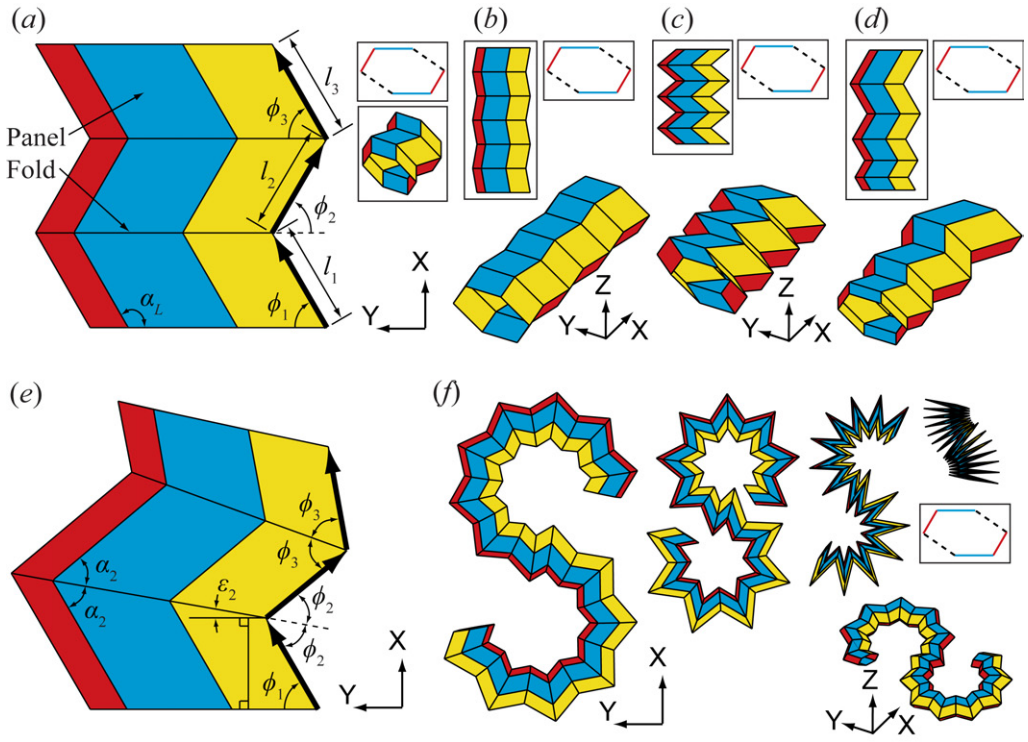


**Figure 5.** (*a*) Cross-section projection in the X-Y direction using a constant projection angle i.e. $\phi = \phi_1 = \phi_2 = \phi_3 = 60°$. (*b*) Constant $\phi = 80°$ projection. (*c*) Constant $\phi = 40°$ projection. (*d*) Constant $\phi = 60°$ projection, with lengths of segment $i$ defined as: $l_i = 0.4 + 0.2 * i$. (*e*) Projection with angle variation. Symmetry between the cross-section and projection vector is preserved in the X-Y plane. (*f*) A rigid foldable S-shaped tube constructed by following symmetry rules in (*e*). All tubes of this figure use the cross-section in figure 2*a*.

The basic type of projection is further extended by allowing an angle shift to occur, where the projection angles are not equal throughout (i.e. $\phi_1 \neq \phi_2 \neq \phi_3 ...$). Figure 5*e* shows the projection where the angle is varied in the $X-Y$ plane. Symmetry is enforced such that the adjacent vertex angles ($\alpha$) about the cross-section are kept symmetric. This projection can be used to create an arbitrary geometry in the $X-Y$ plane that is flat and rigid foldable.

## (b) Projections for rigid, but non-flat foldable origami tubes

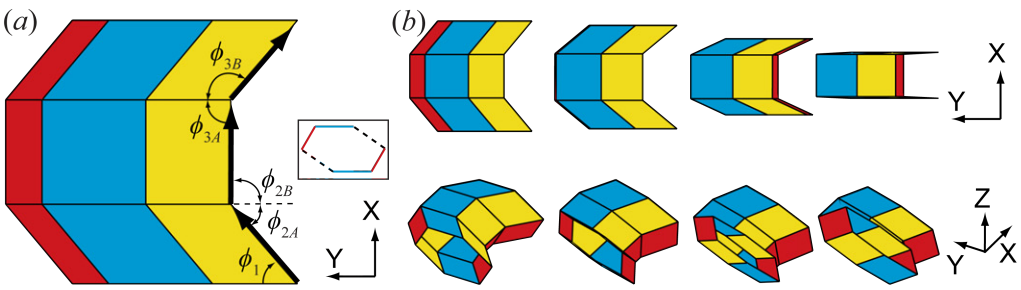


**Figure 6.** (*a*) Cross-section projection in the X-Y direction that does not preserve symmetry about the cross-section i.e. $\phi_{2A} \neq \phi_{2B}$. (*b*) The folding sequence of the non-symmetric projection shown in top and isometric views. The structure cannot fold completely flat.

Projection in $X-Y$ space can also be performed without following the symmetry about the cross-section. In figure 6 we show a projection where the projection angles are $\phi_{2A} \neq \phi_{2B}$, and thus the adjacent vertex angles are also not symmetric. The system can undergo rigid folding, but in this case the folding sequence is restricted and the system cannot fold into a completely flat space (figure 6*b* and Appendix A).

## (c) Extended projections for origami tubes

The final form of projection discussed here is the most general, where the projection is performed arbitrarily in all three dimensions ($X-Y-Z$). The vector can be varied in all directions simultaneously, by using an angle $\phi$ to describe the projection vector in $X-Y$, and $\gamma$ to vary the projection vector in $Y-Z$. Symmetry of the projection is preserved, such that the adjacent vertex angles on opposing sides of a cross-section are equal. This symmetry can be visualized as mirroring the structure locally, which is shown using transparent planes in figure 7*a-c*. For the polygonal cross-section, when this projection is used, the resulting structure is not foldable, and so it is essentially no longer origami, but a static fully restrained structure (Appendix A). However, if a simple symmetric cross-section is used, the structure remains rigid and flat foldable. The structure in figure 7*d* follows an arbitrary spiral in three dimensional space.

# 4. Kinematics in reconfiguring polygonal tubes

The folding of the tube can be preformed through an analytical [34–37] or numerical method [38], by changing a fold angle in one vertex, calculating the other angles in the vertex, and cycling through all of the vertices in the pattern until all fold angles, and the new geometric shape are calculated. We use the numerical method in [38] to perform the folding. In contrast to more simple tube structures, the geometry of the tubes presented here can be reconfigured. Figure 8 shows the two basic geometry reconfigurations that can be obtained from the simple six-sided origami tube. The initially flat in $Y-Z$ segments, can be used as *switches* to change the structural geometry.

A binary system is used to inform the directional change in cross-section and new geometry. The upper and lower switches are defined as a 0 or a 1 and indicate negative or positive slope change in the cross-section respectively (*valley* or *mountain* fold respectively between the first and second panels). The assignment on the upper and lower segments must match to preserve the translational symmetry in equation (2.1), thus if the [U: 1] then [L: 1] as well. In figure 9*a* we extend these definitions to the eight-sided tube from figure 2*d*.

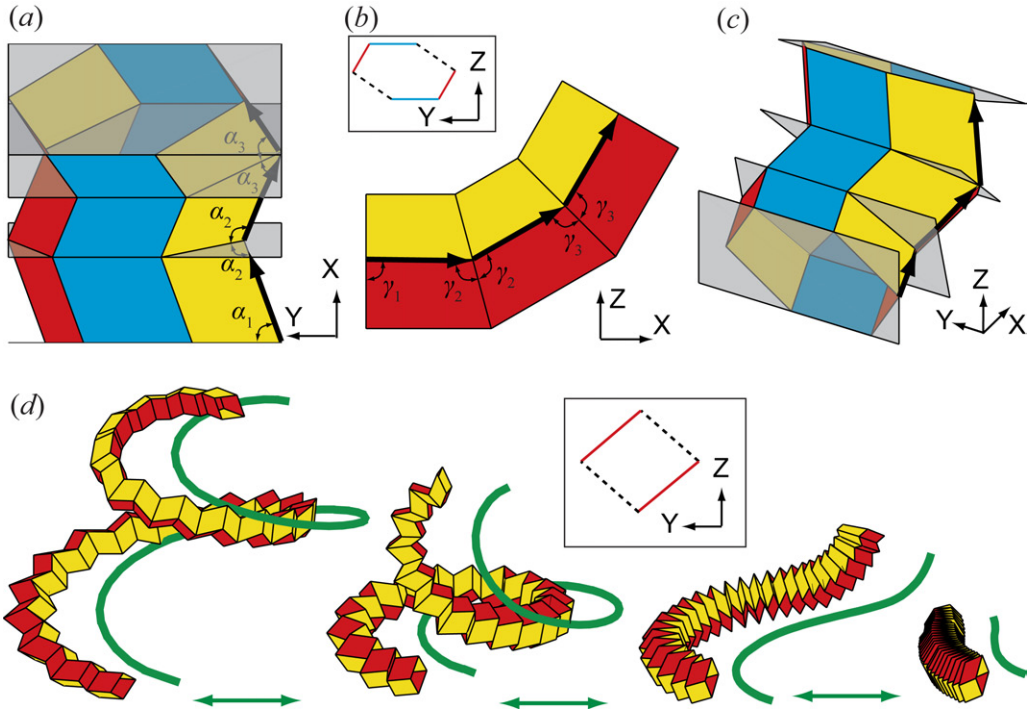


**Figure 7.** Cross-section projection varied in the X-Y-Z directions simultaneously while preserving symmetry of the structure about the cross-section. Projection of six-sided polygon shown in (*a*) top, (*b*) side, and (*c*) isometric views. This polygonal tube cannot fold. (*d*) Folding sequence of four-sided origami tube constructed by projecting along a spiral in three dimensional space. This tube is rigid and flat foldable.

The eight-sided tube has two switches of equal length on both the upper and lower sections. The number of positive switches (1s) on the upper section has to correspond to the number of positive switches on the lower section of the tube. Thus the sum ($k$) of the $L$ and $U$ switches must match. Figure 9*a* shows the six possible switch variations for the eight-sided tube. The number of possible ways to reconfigure the upper section only, follows a binomial coefficient as:

$$\binom{n}{k} = \frac{n!}{k!(n-k)!}, \tag{4.1}$$

where we have $n$ available switches and we want exactly $k$ of them to be positive. For example in figure 9*a* there is only one possible way to reach a total of either $k = 2$ or $k = 0$, configurations I and II respectively. However, there are two possible ways to reach a total of $k = 1$, i.e. [U: 1 0] and [U: 0 1]. Because each variation of the upper section can be coupled with a corresponding lower section with the same polarity sum ($k$), we need to take the square of these possibilities, and sum them to find the total number of possible variations for the cross-section. This results in the central binomial coefficient:

$$\sum_{k=0}^{n} \left( \frac{n!}{k!(n-k)!} \right)^2 = \frac{(2n)!}{(n!)^2}. \tag{4.2}$$

This function gives the total number of unique cross-section variations that can be obtained when folding a reconfigurable tube with $n$ flat segments or switches. The possible upper section assignments for a $n = 2$ and $n = 3$ tube are shown in figure 9*b*. The number of possible upper section variations follow Pascal's triangle (figure 9*c*), and the total number of possible configurations follow the central binomial coefficient (figure 9*d*). The most basic, four sided tube

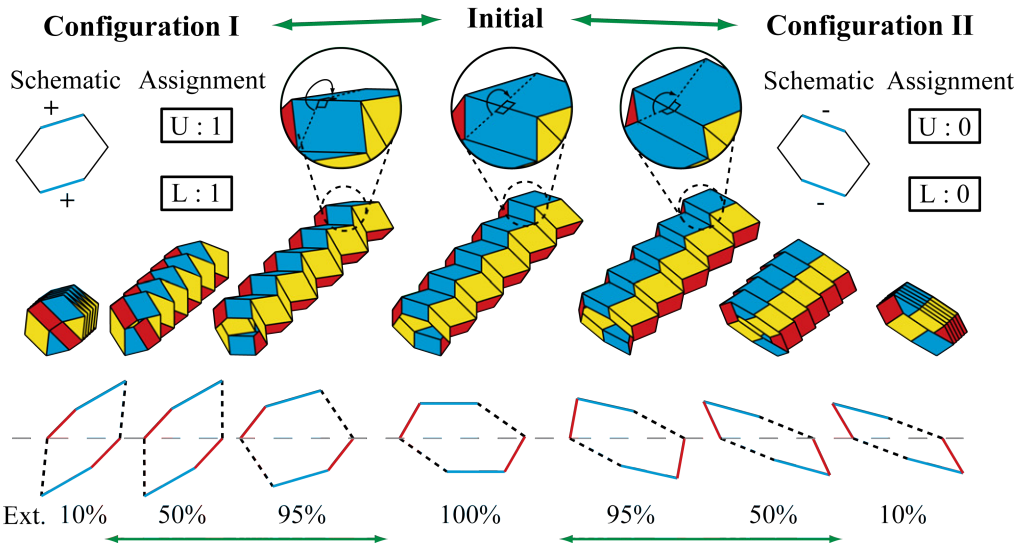


**Figure 8.** The six-sided tube can be folded into two different configurations by changing the polarity of folds (valley or mountain) on the single flat segment ($n = 1$). A cross-section schematic with positive or negative slopes is used to inform the fold assignment for the first/last fold (0 = valley, 1 = mountain). The folded cross-sections of the two configurations are not symmetric because edge groups $a$ and $c$ in the cross-section definition are not symmetric (figure 2*a*).

cross-section (e.g. figure 7*d*) has no switches ($n = 0$), and thus has only one possible cross-section configuration. On the other hand, the tube with four symmetric switches ($n = 4$) shown in figure 1 can reconfigure into 70 distinct cross-sections.

## 5. Cellular extensions for reconfigurable origami tubes

The projection technique for creating polygonal tubes can be extended to creating cellular assemblages that have similar geometric characteristics. When the translational symmetry is used in the cross-section(s) and an admissible projection is followed to construct the three dimensional structure, the folding and reconfigurable characteristics remain similar to before. In figure 10 we show two assemblages that use a constant angle projection, although it is possible to use more advanced curved projections as well. The cross-section in figure 10*a* is created by discretizing the cross-section into smaller sections. All of the internal cross-sections, as well as the global external cross-section, follow the translational symmetric rules in equation (2.1). This assemblage can still be reconfigured as shown in figure 8. In figure 10*b* we combine four tubes together, two of which have reconfigurable cross-sections. This assemblage can now be reconfigured into four different cross-sections, with configurations III and IV being rotationally symmetric. A variety of new assemblages can be constructed using these ideas, however the initial cross-sections cannot have overlapping components, and the kinematics of reconfigurations should be carefully analysed. When multiple tubes and cross-sections are reconfigured, it may be possible for different components to experience interaction or contact, and some of the reconfigurations may be obstructed.

Polygonal origami assemblages can be further enhanced by using different projection angles and projection directions, for the different tubes within the assemblage [13,39]. The most interesting case is a *zipper* coupling of tubes, where a positive projection $\phi$ is used for one tube and a negative $\phi$ for another. These zipper assemblages can be used to create significantly stiffer thin sheet origami structures. The assemblages can be generalized in numerous ways, but they also limit some of the projection directions that can be used to create the system [39]. Furthermore, it is possible to introduce techniques for locking the origami configuration into a sandwich-like

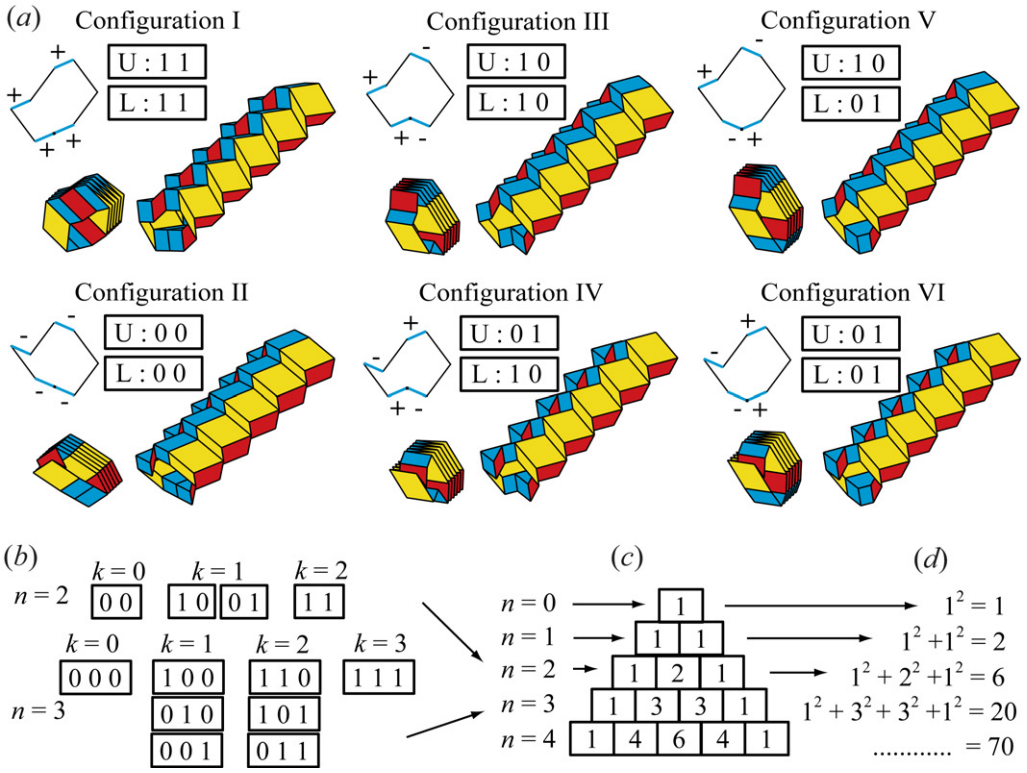


**Figure 9.** Variations in reconfiguring polygonal tubes. (*a*) An eight-sided tube with two equal length segments (switches) can reconfigure into six unique configurations. The three dimensional models are shown at 10% and 95% extension. (*b*) Possible switch variations for the upper section only, with $n = 2$ and $n = 3$ switches. The variable $k$ corresponds to the sum of the of switch assignments. (*c*) A Pascal's triangle shows the number of variations for the upper section of the tube only. This is the binomial coefficient with $n$ representing the rows and $k$ the columns. (*d*) The total number of possible cross-section configurations. This is equivalent to the central binomial coefficient.

structure [11,40]. These additions can enhance the structural rigidity of the systems, but can restrict the deployment and reconfigurable kinematics of the polygonal tubes. Future research can explore the numerous assemblage variations proposed and determine useful methods for enhancing the mechanical characteristics of the structures.

## 6. Elastic behaviour of polygonal tubes

In this section, we explore the global mechanical characteristics of the tubes with a finite-element (FE) analysis software (Abaqus [41]). Each of the origami panels is discretized with $8 \times 8$ shell elements and the folds are modelled using rotational hinges as shown in figure 11. The model uses standard S4 general purpose shell elements with finite membrane strains that are appropriate for the small deformation analyses of the thin sheet origami structures. We model the eight-sided reconfigurable tube from figure 2*d*. The cross-section edges for the upper section have slopes of $[\theta_a, \theta_b, \theta_c] = [30, 90, 125]^\circ$, and lengths of $[b_{U1}, a_{U1}, b_{U2}, c_{U1}] = [0.5, 0.7, 0.5, 1]$ cm. The tube is ten segments long, and is created with constant projection of $\phi = 60^\circ$ and $l = 1$ cm. The configuration of the structure is defined based on the idealized zero-thickness rigid kinematics, however, to define the stiffness of the structure we assign a thickness of 0.1 mm which translates to roughly $L/t \approx 50 - 100$. The model does not however account for detailed effects of the thickness such as intersection that may occur when we attempt to fold an origami with finite thickness.

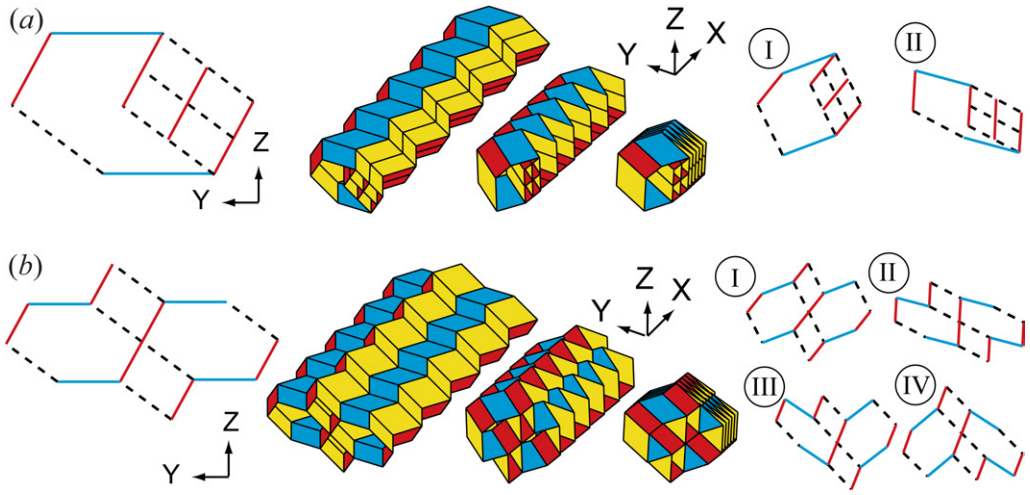


**Figure 10.** Cross-sections, isometric folding sequence and possible reconfigured cross-sections of cellular origami assemblages. (*a*) The basic six-sided polygon has four smaller parallelogram tubes inserted within. This assemblage has two possible configurations similar to before. (*b*) Assemblage consisting of two six-sided and two four-sided tubes together. This structure can reconfigure into four states.

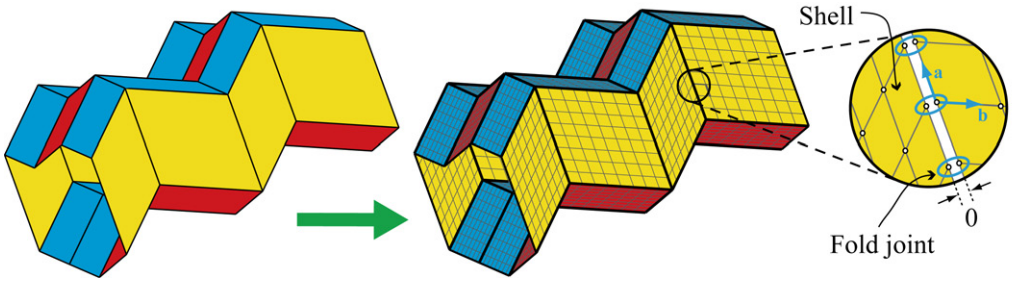


**Figure 11.** A portion of the eight-sided reconfigurable tube with the corresponding FE discretization. The inset shows the localized zero-length connectivity at the fold lines.

Other model parameters are defined as Young's modulus $E = 5$ GPa, Poisson's ratio $\nu = 0.33$, and density $\rho = 650$ kg/cm$^3$. In reality the behaviour and stiffness of the fold lines can depend on the material and fabrication used to make the origami. Here, we assume linear elastic folds where the stiffness for a rotation of $\rho$ radians is specified as $K_\rho = 0.0164$ N*cm/rad per one centimetre of fold line. The fold lines are assumed to be more flexible in bending than the panels, and thus $K_\rho$ is specified to be one tenth (1/10) the bending stiffness of an origami panel with a diagonal length of one centimetre. The dimensions and units used here are chosen arbitrarily but within a realistic range to give qualitative insight to the origami behaviour. Quantitative results for engineered origami systems could be obtained using known dimensions and material properties. The analytical model captures the elastic behaviours of origami type structures: 1) panels stretching and shearing, 2) panels bending, and 3) bending along prescribed fold lines. We have evaluated the mesh convergence for the tube when it is loaded as a cantilever later in this section. The $8 \times 8$ shell mesh approximates displacements within 4% of a significantly finer mesh discretized with $32 \times 32$shell elements per panel. In this paper, we use elastic and small displacement approximations for all analyses. Future research will be needed to understand localized behaviours in origami structures, as well as the large displacement behaviours which could be of significant importance.

We use an eigenvalue analysis to explore the global mechanical properties of the reconfigurable origami tube. These analyses can be used to determine how flexible or stiff the structure would be for bending, twisting or other deformations. We obtain the eigenvalues $\lambda_i$ and corresponding eigen-modes $\mathbf{v}_i$ of the structure using a linear dynamics system of equations $\mathbf{K}\mathbf{v}_i = \lambda_i \mathbf{M}\mathbf{v}_i$ where ($\mathbf{K}$) is the stiffness matrix and ($\mathbf{M}$) is the mass matrix of the structure. The eigenvalues are arranged in an incremental order ($i$) and represent the excitation frequencies that would deform the structure into the corresponding eigen-mode. The eigenvalues are also proportional to the total energy of each eigen-mode (elastic strain energy and kinetic energy), meaning that eigen-modes with higher eigenvalues require more energy to achieve the given deformation. The structure is analysed with no boundary conditions, thus the first six eigenvalues are zero, with eigen-modes representing rigid body motion of the structure in three-dimensional space (three displacement and three rotational modes). We start considering the seventh and subsequent eigen-modes of the structure.

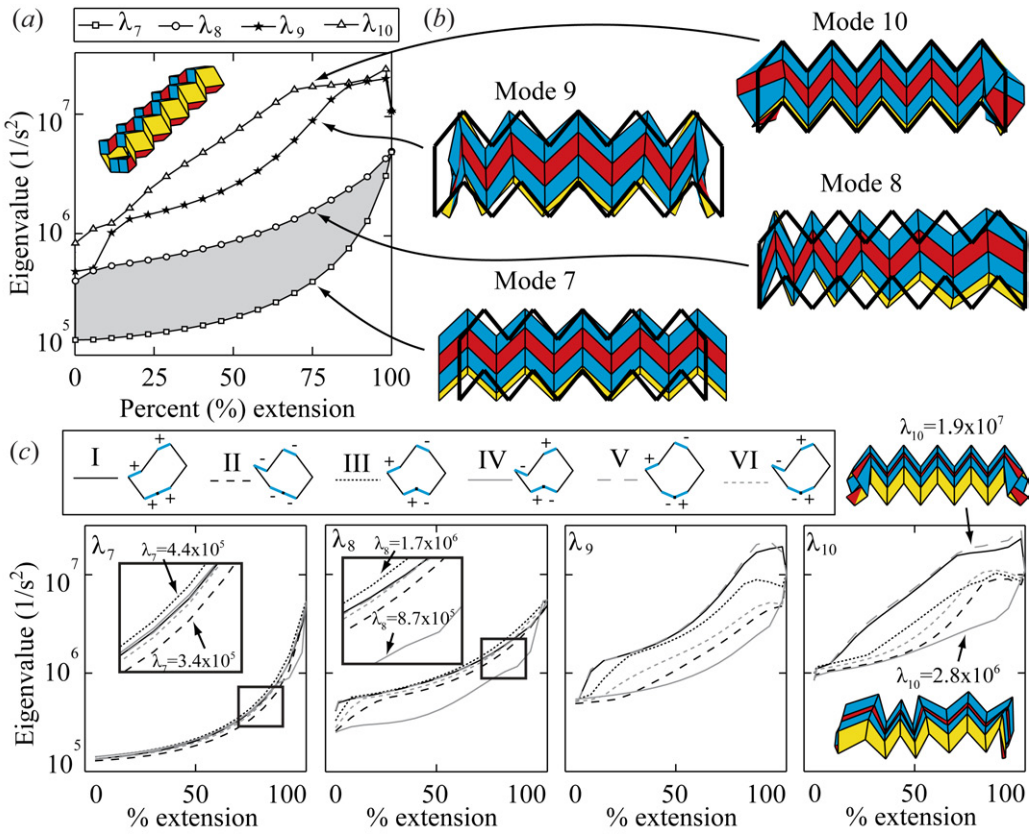


**Figure 12.** Eigenvalue analyses of eight-sided reconfigurable tube with two switches presented in figure 9. (*a*) Eigenvalue versus the extension of the tube in configuration I. (*b*) Corresponding eigen-modes at 75% extension. (*c*) Eigenvalues seven through ten presented for each of the six possible geometric reconfigurations of the tube.

For the eight-sided reconfigurable tube the seventh eigen-mode follows the kinematic folding and unfolding of the structure (figure 12*a-b*). The seventh mode has the least energy indicating that it is easiest to deform the structure by following the prescribed folding sequence. The eight mode is a squeezing mode, where one end of the tube is folding and the other end is unfolding. By changing the geometry or through tube coupling described in Section 5 it could be possible to substantially increase the band-gap $\lambda_8 - \lambda_7$, creating a structure that is easy to deploy,

but is substantially stiffer for other deformations. The ninth mode of the structure is another manifestation of squeezing with the centre unfolding and the ends folding . The tenth mode is a localized mode, where the panels at the end of the tube fold. The ninth and tenth eigenvalues are substantially higher, meaning the structure is stiffer for these and other types of deformations.

Because the geometry of the system changes, the magnitudes of the eigenvalues also change with respect to the extension of the system. Extension here is defined as a percentage of the fully extended length. When the structure is at 0% extension it is completely folded down, while at a 100% extension the switches flatten and the system can be reconfigured. The eigenvalues for rigid folding and squeezing remain essentially the same regardless of the folded configuration, although there are some small differences in magnitude. However, the ninth and tenth mode are greatly affected by the different folding configurations (figure 12*c*). This is because the cross-sectional geometry has a higher influence in determining the more complex localized and global bending modes.

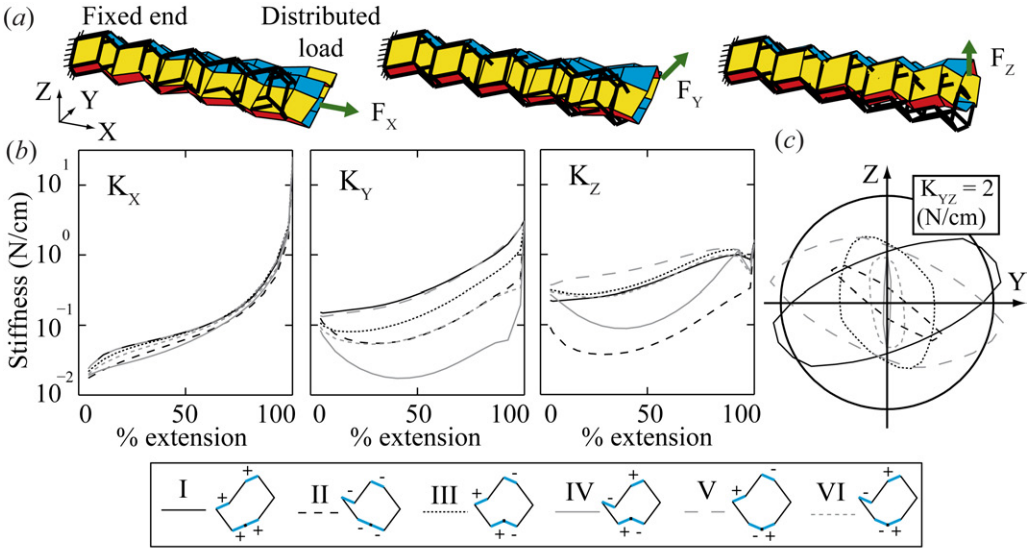


**Figure 13.** Structural cantilever analyses of eight-sided tube. (*a*) Representative deformed shapes scaled $\times 1000$ for the tube in configuration I at 95% extension. (*b*) The stiffness of different tube configurations in the three Cartesian directions with respect to the extension. (*c*) The tube stiffness for different loading directions in the $Y - Z$ plane represented as a radial plot. The tubes are at an extension of 95%.

In figure 13 we present a cantilever analysis of the eight-sided tube in different configurations. One end of the cantilever is fixed and a small uniformly distributed load (summing to a total of 0.001 N, e.g. $F_X = 0.001$ N) is applied on the other end. We perform static, linear elastic, small displacement analyses of the structures, with the main objective of exploring the global bahaviours and anisotropy of the tubes. The system displacements ($\Delta_X$, $\Delta_Y$, $\Delta_Z$) are calculated using the equation $\mathbf{F} = \mathbf{K}\Delta$, where $\mathbf{F}$ is a vector of forces. Subsequently, the system stiffness is calculated as $K_X = F_X/\delta_X$, where $\delta_X$ is the mean $X$ direction displacement of the loaded nodes. A squeezing type deformation occurs for some of the loaded cases, and this is believed to result in lower stiffness than if the origami was engaged in stretching and shearing. Different cross-section configurations, can have drastically varying stiffness characteristics, with up to an order of magnitude between different cross-sections (figure 13*b*). Typically, configurations I and V are the stiffest while configurations II and IV are the most flexible. We also show the stiffness perpendicular to the $X$ axis, as a radial plot in figure 13*c*. The I and V configurations have large oval plots, meaning they have relatively higher stiffness in most directions. Each

of the cross-sections also has a different direction (in $Y-Z$) where it has a lower or higher stiffness. This phenomena indicates that the reconfigurable tubes have a highly adjustable anisotropy when used as cantilevers. The behaviours observed in this section show that the cross-section geometry can have a significant influence on the mechanical properties of the system. Thus, the reconfigurable polygonal tubes can be used to create highly tunable and adaptive structural systems. Detailed research is needed in this area to determine the influence of different cross-section geometries, as well as the tunability achieved from each reconfiguration.

## 7. Cylindrical origami tubes

We explore a uniform circular pipe (made from a thin sheet) experiencing uniform out-of-plane loading and compare it with similar origami tubes. Figure 14*a* shows the pipe that is $L = 10$ cm long, loaded in space with symmetric out-of-plane distributed load equal to $F/L$. In this section, we use a total force of $F = 0.001$ N, and we assume linear elastic, small displacement behaviours. The radius of the pipe is $r = 2$ cm, and all other parameters (i.e. $t$ and $E$) are the same as for the origami analysis in Section 6. An analytical solution for this problem is found using Castigliano's theorem where the pipe is simplified to a two dimensional bending of a thin beam (Appendix B). The total diametric deflection ($\delta_d$), coaxial with the applied load, is found to be

$$\delta_d = \left(\frac{\pi}{4} - \frac{2}{\pi}\right)\frac{12Fr^3}{ELt^3} = 0.00286 \text{ cm}. \tag{7.1}$$

Subsequently, we preform similar analyses on the origami tubes with the same parameters, and dimensions defined to match the pipe as closely as possible. All cross-sectional edge lengths are defined as $2\pi r/N_{Edge}$ where $N_{Edge}$ are the total number of edges on the circular tube. As such, the tube perimeter is the same as the analytical case. The edges are arranged in a symmetric fashion so that the cross-section becomes a regular polygon (figure 14*b*). Three cases with $N_{Edge} =$ 6, 10, and 14 are used, such that there is a single flat segment in the initial configuration, meaning that the initial configuration is the fully deployed state. The number of panels in the $X$ direction is chosen as 6, 8 and 12 for the three cases respectively, so that the structure is symmetric and the panels are approximately square. The projection angle defining the three dimensional shape is varied, and a consistent projection length is used so that the origami tube is $L = 10$ cm long in the fully deployed (same as initial) configuration. We perform a static analysis by loading the vertices on the top flat segment with a downward force, such that the edge vertices carry half the load of the internal vertices (grey versus black triangles in figure 14*b*). The loads are defined such that the total applied load sums to $F = 0.001$ N. The bottom vertices of the tubes are restrained in the $Z$ direction, representing a symmetric loading similar to figure 14*a*.

We use static, linear elastic, small displacement analyses to evaluate the mechanical properties of the origami tubes. Scaled deformed shapes of $N_{Edge} = 10$ tubes with two different projection angles are shown in figure 14*c-d*. The tube with $\phi = 65^\circ$ is much stiffer and has an irregular deformed shape where panels bend and stretch. The tube with $\phi = 85^\circ$ has a more regular deformed shape, similar to what we would expect from a thin pipe, and in this case, deformation occurs primarily by bending along the longitudinal fold lines. Stiffness with respect to the projection angle $\phi$, of the tubes with different $N_{Edge}$ is shown in figure 14*e*. The origami stiffness is calculated as in Section 6, and the analytical stiffness solution for the circular pipe is calculated as $F/\delta_d$. Similar to the deformed shapes, tubes with lower projection angles have lower displacement and are stiffer, while tubes with a projection angle close to $90^\circ$ are more flexible because they permit folding along the longitudinally oriented fold lines. The origami tubes with projection angles between $\phi = 45^\circ - 75^\circ$ are stiffer than the analytical solution for a circular pipe. This behaviour is similar to that of corrugated pipes and sheets [42]. Corrugated pipes have a higher stiffness for out-of-plane loadings, which makes them suitable for many applications such as culverts. Tubes with more edges e.g. $N_{Edge} = 14$ have more fold lines along their cross-section perimeter, making them more flexible. The results are verified with physical models (figure 14*f-h*). The stiffness of the fold lines $R_{FP}$ factor, does not influence the deflection significantly for cases

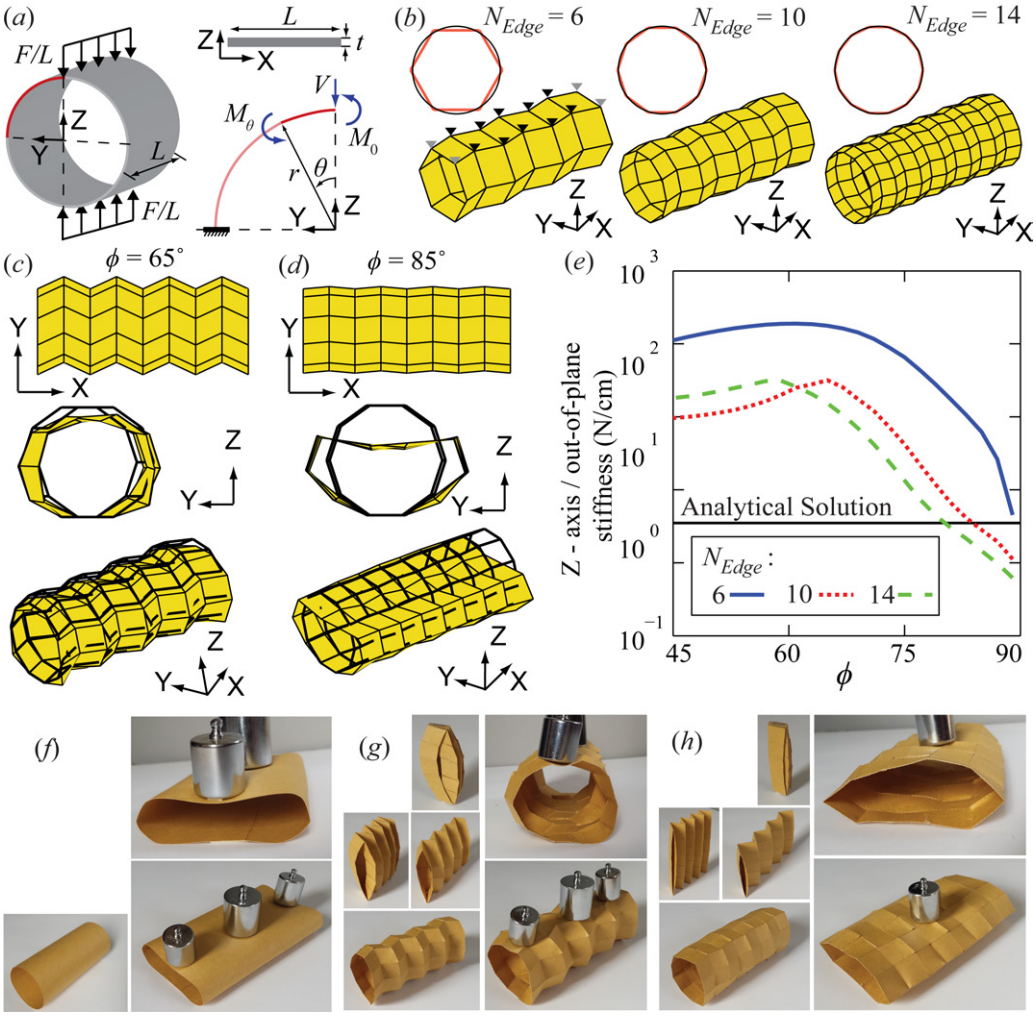


**Figure 14.** Out-of-plane compression on a pipe. (*a*) Problem definition and analytical approximations (Appendix B). (*b*) Origami tubes with $N_{Edge} = 6$, 10, and 14. The origami tube cross-sections are overlayed with a $r = 2$ cm circle. The loading is only shown for the $N_{Edge} = 6$ tube. (*c*) A $\phi = 65^\circ$ tube, and (*d*) a $\phi = 85^\circ$ tube with $N_{Edge} = 10$. The top (X-Y) view is shown as a reference and the lower views show the deformed shapes. The deformed shapes are scaled $\times 10000$ for the stiffer $\phi = 65^\circ$ tube and $\times 200$ for the more flexible $\phi = 85^\circ$ tube. (*e*) The out-of-plane stiffness of tubes versus the projection angle $\phi$. (*f-h*) Physical models of a uniform sheet, $\phi = 65^\circ$, and $\phi = 85^\circ$ tubes respectively, loaded out-of-plane with 400 grams. The $\phi = 85^\circ$ tube is only loaded with one 100 gram weight due to the much larger deformation.

with lower projection angle $\phi < 75^\circ$. However, for higher $\phi$ the fold lines are the primary location of deflections, and thus their stiffness greatly affects the tube stiffness.

## 8. Concluding remarks

We introduce a new category of origami tubes that have reconfigurable polygonal cross-sections. The tubes are rigid and flat foldable, and have a continuous perimeter. The cross-sections of the tubes can be a wide variety of convex or non-convex polygonal shapes that follow translational symmetry. Projection is used to define the three dimensional shape of the tube, but non-admissible (e.g. non-symmetric) projections, may limit the flat and rigid foldability of the system. The cross-section geometry can contain any number of $n$ switches that can be used like binary bits to

program the geometric reconfiguration of the cross-section. We show that the total number of possible cross-section variations for a tube follow the central binomial coefficient of $n$. A cellular cross-section or coupling of multiple tubes can be used to create a new variety of assemblages that enhance the functionality and reconfigurable properties of the tubes.

In addition to the geometric variations and reconfigurable kinematics, this paper also explores some mechanical properties of the polygonal tubes. We show that the tubes have only one flexible mode for kinematic deployment for which the stiffness is not significantly influenced by reconfiguring the cross-section. On the other hand, the cross-section configuration can influence other deformation modes and the out-of-plane stiffness of the tubes. This property can be used to make tunable structures that can change their mechanical properties. If the origami tubes are used as circular pipes, they can be designed to have a high out-of-plane stiffness similar to that of corrugated pipes. An appendix proposes future research directions on applications, fabrication, and non-linear deformations, all of which will enhance the practicality, functionality and capability of the reconfigurable tubes. We envision that the physical attributes, versatility, and programmable characteristics of the polygonal origami tubes will enable solutions of varying scale in science and engineering.

Data accessibility statement. The work does not have any experimental data.

Competing interests statement. We have no competing interests.

Authors' contributions. ETF, GHP and TT designed the research, conceived the geometric designs and computational models, interpreted the results, and wrote the paper. All authors gave final approval for publication.

Funding statement. This research was partially supported by the National Science Foundation (NSF) grant CMMI 1538830. The authors also acknowledge support from the NSF Graduate Research Fellowship; Japan Society for the Promotion of Science Fellowship; Raymond Allen Jones Chair at the Georgia Institute of Technology; and Japan Science and Technology Agency Presto program.

Ethics statement. This work did not involve any human data.

## Appendix A. Foldability of origami tubes

In this appendix we verify the developability, flat foldability and initial rigid foldability using the approach introduced by Tachi [43]. We assume that the origami panels have an infinitesimally small or zero-thickness to satisfy the mathematical definitions. The origami tubes defined by Sections 2 and 3 contain a total number of $n^{vert}$ internal vertices where four fold lines meet, and a number of $n^{panel}$ four-sided panels. The folding characteristics of the origami can be explored by performing the following vector calculations for the vertices and panels:

$$\mathbf{c}^{\text{dev}} = \left[ 2\pi - \sum_{k=1}^{4} \alpha_{k,i} \right]_{n^{vert}\times 1} = \mathbf{0}, \tag{8.1}$$

$$\mathbf{c}^{\text{flat}} = \left[ \sum_{k=1}^{4} (-1)^k \alpha_{k,i} \right]_{n^{vert}\times 1} = \mathbf{0}, \tag{8.2}$$

$$\mathbf{c}^{\text{planar}} = \left[ \rho_j \right]_{n^{panel}\times 1} = \mathbf{0}, \tag{8.3}$$

where $\alpha_{k,i}$ represents the $k$-th vertex angle in the $i$-th vertex, and $\rho_j$ represents the dihedral angle between the normals of two triangles that together create the $j$-th panel of the tube. When $\mathbf{c}^{\text{dev}} = \mathbf{0}$ for all vertices, then the origami is developable, meaning it can be created from a single flat piece of material. The origami tubes presented here have mostly non-developable vertices, and thus they cannot be folded from a single flat piece of material. However, some of the vertices may be developable and thus a portion of the tube may be constructed from an initially flat sheet (e.g.

the single four-sided tube can be constructed from two flat sheets [28]). When $\mathbf{c}^{\text{flat}} = \mathbf{0}$, then all vertices of the origami are flat foldable meaning that, they can fold down to a flat 2 dimensional state. The definitions in Section 3(a) and 3(c) intentionally ensure symmetry when preforming a projection of the cross-section, thus they ensure that all vertices are flat foldable. However, in Section 3(b) where symmetry is not preserved, we loose the flat foldability ($\mathbf{c}^{\text{flat}} \neq \mathbf{0}$). Equation

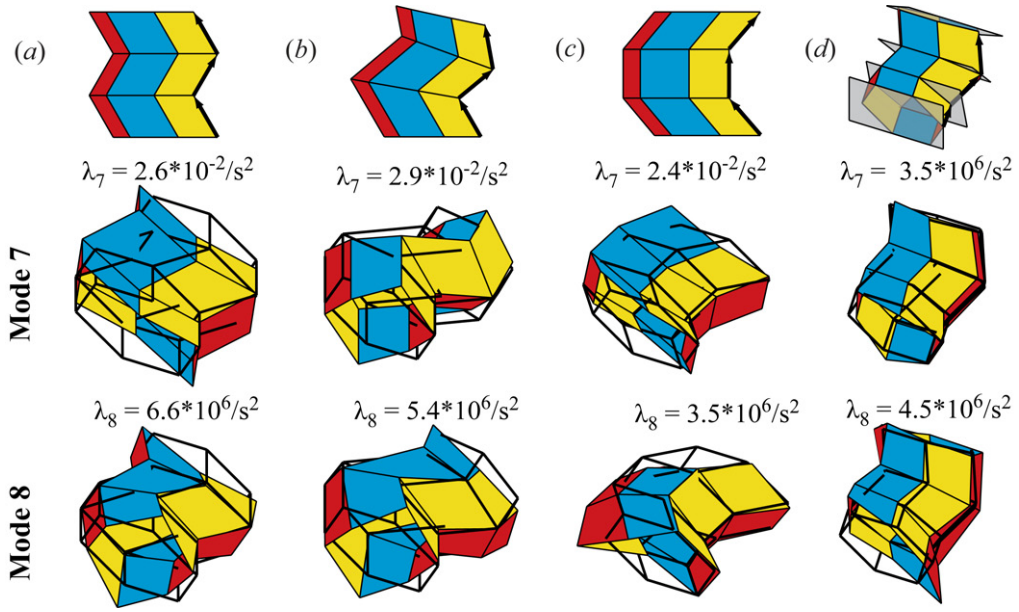


**Figure 15.** Schematic (top row), seventh mode (middle row) , and eighth mode (bottom row), of basic projection definitions. (*a*) Constant angle projection in $X-Y$. (*b*) Projection in $X-Y$ with symmetry enforced. (*c*) Projection in $X-Y$ without preserving symmetry. (*d*) Simultaneous projection in $X-Y-Z$. Low eigenvalues correspond to a soft, rigid folding mode of the origami.

(8.3) indicates that all panels are planar or flat for a given configuration. The dihedral angle ($\rho_j$) can be calculated using the four nodes on the corners of the panel, and will always equal 0 at the initial projected configurations defined using Section 3. Thus all tubes satisfy $\mathbf{c}^{\text{planar}} = \mathbf{0}$, however, this is only a necessary condition for rigid foldability and is not sufficient. For rigid foldability, folding along fold lines should permit the structure to transition between states while $\mathbf{c}^{\text{planar}} = \mathbf{0}$ is continuously satisfied. Analytical derivations of the kinematics and geometric characteristics of foldability (including rigid foldability) have been previously discussed [34–37], however these tend to be cumbersome for verifying the rigid foldability of complex origami systems. A more straightforward method to check rigid foldability, is to perform the eigenvalue analyses described in Section 6 with the fold stiffness ($K_\rho$) substantially reduced (e.g. to $10^{-7}$) representing fold lines with no stiffness. In these analyses, the seventh and possibly higher eigenvalues will be near zero, indicating a rigid folding motion where a kinematic transition is permitted by folding along the fold lines. Figure 15 shows the eigenvalues and eigen-modes for the basic origami assemblies studied in this paper. All cases except symmetric $X-Y-Z$ projection have a $\lambda_7$ that is low ($\approx 10^{-2}$), indicating a rigid folding motion. For the $X-Y-Z$ projection case, $\lambda_7$ is of much higher order indicating that bending of the panels must occur to deform the structure, and that the tube does not have a rigid folding mode. For the structures in figure 15*a-c*, $\lambda_8$ is substantially higher than $\lambda_7$ indicating that only one rigid folding motion exists, these systems can be classified as *one degree of freedom* for rigid folding.

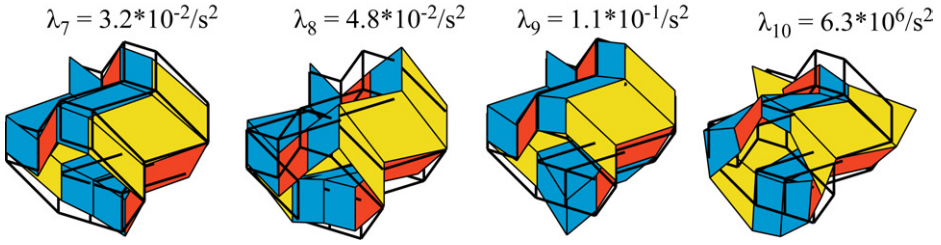


**Figure 16.** The seventh to tenth eigenvalues and eigen-modes of the eight-sided tube when it is at a fully extended state. Mode seven corresponds to configuration II and is the symmetric inverse to configuration I; Mode eight is corresponds to configuration IV and is symmetric to V; and Mode nine corresponds to configuration VI and is symmetric to III. Mode ten is the squeezing mode.

In figure 16 we show the eigenvalue and eigen-modes of the eight-sided tube with two switches ($n = 2$). Curiously, for this case, the system has three soft modes where the rigid folding can occur, and the tenth mode is the first to engage the origami panels in bending. These rigid folding modes each correspond to one of the system configurations shown in figure 9, and each one of them also has a symmetric inverse that corresponds to another system configuration. These results indicate that the system has three non-symmetric degrees of freedom for rigid folding. However, once the structure enters one of the folding configurations (extension < 100%), it behaves like a one degree of freedom system, where it only has a single flexible mode for rigid folding (figure 12). This phenomena of the eight-sided tube is similar to a flat sheet that can enter numerous different folding patterns when initially folded. Future, research could investigate differences in rigid folding configurations, the symmetric inverse eigen-modes, and the varying programmability possible with the polygonal tubes.

## Appendix B. Analytical solution for a pipe loaded out-of-plane

The exact analytical solution for the out-of-plane bending of a pipe can be calculated using Castigliano's theorem where we simplify the problem to a two dimensional bending of a thin curved beam. The theorem states that the displacement $\delta_q$ at the point where a load $Q$ is applied can be found by

$$\delta_q = \frac{\partial \mathbf{U}}{\partial Q} = \int_0^l \frac{M_x}{EI}\frac{\partial M_x}{\partial Q}dx, \tag{8.4}$$

where $\mathbf{U}$ is the elastic strain energy, $M_x$ is the bending moment, $I$ is the area moment of inertia, and $x$ is the distance along the beam. By using symmetry, we only consider a quadrant of the pipe's cross-section which is loaded with a force $V = F/2$ (figure 14*a*). The idealized thin beam has a width equal to the length of the pipe $L$ ($X$ direction), and a depth of $t$ in the bending axis (perpendicular to $X$), resulting in the area moment of inertia $I = Lt^3/12$. A point along the beam is defined as a function of the angle $\theta$, and the bending moment ($M_\theta$) and the partial derivatives are calculated as

$$M_\theta = Vr\sin\theta - M_0, \qquad \frac{\partial M_\theta}{\partial V} = r\sin\theta, \qquad \frac{\partial M_\theta}{\partial M_0} = -1. \tag{8.5}$$

Using the theorem we can now calculate

$$\delta_{M_0} = \int_0^l \frac{M_x}{EI}\frac{\partial M_x}{\partial M_0}dx = \frac{1}{EI}\int_0^{\pi/2}(Vr\sin\theta - M_0)*(-1)*rd\theta = \left(\frac{\pi}{2}M_0 - Vr\right)\frac{r}{EI}, \tag{8.6}$$

$$\delta_V = \int_0^l \frac{M_x}{EI}\frac{\partial M_x}{\partial V}dx = \frac{1}{EI}\int_0^{\pi/2}(Vr\sin\theta - M_0)*r\sin\theta*rd\theta = \left(\frac{\pi}{4}Vr - M_0\right)\frac{r^2}{EI}. \tag{8.7}$$

By enforcing symmetry, the rotation at the unrestrained end of the beam will be $M_0 = 0$, and using equation (8.6) we find that $M_0 = 2Vr/\pi$. Substituting $M_0$ into equation (8.7), the total diametric

deflection coaxial with the applied load is found to be

$$2\delta_V = 2\left(\frac{\pi}{4} - \frac{2}{\pi}\right)\frac{Vr^3}{EI} = \left(\frac{\pi}{4} - \frac{2}{\pi}\right)\frac{12Fr^3}{ELt^3}. \tag{8.8}$$

If we wish to find the total diametric deflection perpendicular with the applied load, we can use a fictitious load $H$ applied horizontally at the free end of the curved beam, and use the same methodology to find

$$2\delta_H = 2\left(\frac{2}{\pi} - \frac{1}{2}\right)\frac{Vr^3}{EI} = \left(\frac{2}{\pi} - \frac{1}{2}\right)\frac{12Fr^3}{ELt^3}. \tag{8.9}$$

# Appendix C. Practical considerations and future extensions for reconfigurable origami tubes

In this appendix we propose future research on the reconfigurable tubes to explore (a) practical applications, (b) considerations for physical fabrication, and (c) non-linear behaviours that can extended capabilities. This section is meant to inform and motivate future research, rather than to provide a holistic discussion on the different topics.

## (a) Practical applications

The polygonal cross-section origami tubes discussed in this paper open up a variety of applications in science and engineering. The continuous perimeter of the cross-sections could enable the tubes to be used in fluid flow applications. More traditional applications would involve primarily using these tubular origami as deployable pipe-like [4,15,16] or bellow systems [17,18]. These could have wide and varied applications including deployable pipes for construction, biomedical devices, or inflatable space structure components. The new projection definitions introduced in Section 3, provide a new capability where the origami tubes can follow a curved profile when deployed, versus the straight profile of previously introduced tubes. An instance taking advantage of this benefit, would be constructing a ventilation system, where the entire origami tube is deployed to carry air through a congested area, rather than connecting multiple straight and curved pipe segments. The properties studied in Section 7, show added benefits where the polygonal tubes have more stiffness for out-of-plane loading, than a conventional pipe with a constant cross-section. This property could allow for the deployable construction of culverts, or other pipes that need to carry large loads.

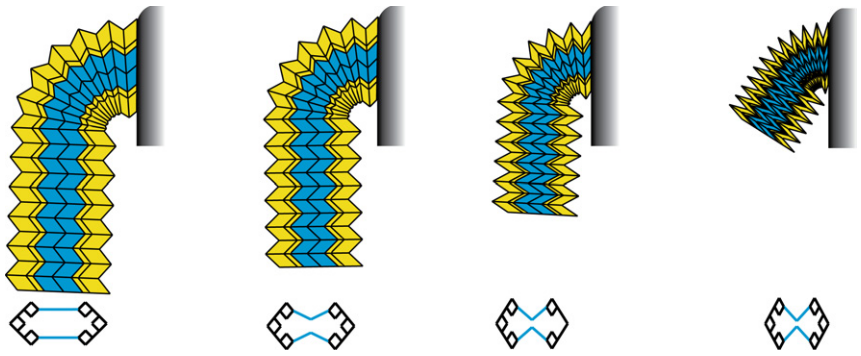

**Figure 17.** Potential application of origami tubes used as a robotic arm with reconfigurable components. The cross-section shown on the bottom reduces in area and could be used as a gripper when the tube is retracting.

The programmable capability of the tube cross-sections offers novel applications where the structure can morph and adapt. The tubes can have an adaptable volume, surface properties,

mechanical characteristics and more, simply through reconfiguring the polygonal cross-section. For example, components placed inside aircraft wing could be used to change the lift and drag properties of the wing for different stages of flight [6]. The variable stiffness properties of the origami tubes discussed in Section 6 could allow for new devices in aerospace, mechanical, and civil engineering. Robotic components, such as the deployable and reconfigurable arm in figure 17 could be designed to simultaneously fulfil multiple functions. A griper can be used with the reconfigurable cross-section, while the cellular divisions could add stiffness and carry electrical wiring, pneumatic tubes, or other utilities (e.g. similar to multi-functional dental tools). Although these applications are still far from reality, they offer many potential advancements from current day engineering approaches.

## (b) Design and fabrication

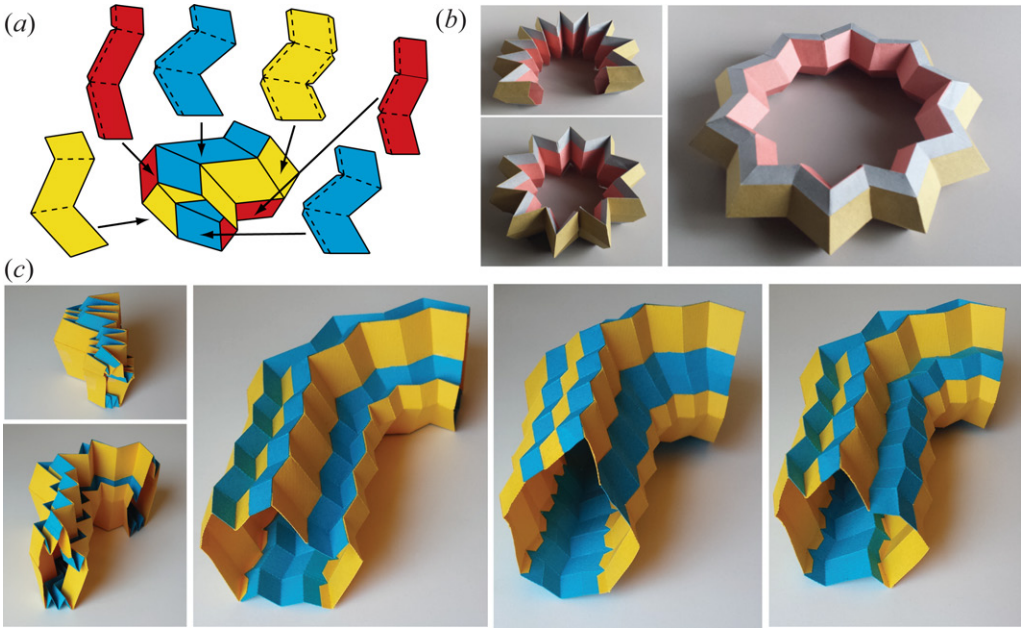


**Figure 18.** (*a*) Strips of panels cut out from flat sheets can be used to construct the three dimensional, non-developable tube. Dashed lines indicate fold lines, and the tabs at the sides of the sheets can be used to attach sheets together. (*b*) Physical model of a six-sided polygonal tube that forms a star when fully deployed (*c*) Physical model of the reconfigurable origami from figure 1 is shown in different configurations. The tabs for attachment are visible on the bottom.

There is currently a tremendous amount of research aimed at making origami feasible for real world applications. The geometric origami design, fabrication methods, materials, and deployment mechanisms, all depend on the scale and function of the origami system. For small applications, origami can be 3D printed with living hinges [44]. More simply however, it is possible to cut out the origami from a flat sheet and fold the system along perforated or etched fold lines. As a proof of concept, we have fabricated several small ($\approx 30$ cm) paper models (figures 14, 18, and 19) to highlight the capabilities of the reconfigurable polygonal tubes. All models are manufactured from 160 g/m$^2$ paper that has an approximate thickness of 0.25 mm. Panel heights and widths vary from 1 to 3 cm, thus maintaining a relatively high length/thickness ratio that is typical for origami. The folds are created by perforating the paper with 0.5 mm cuts spaced evenly at 1 mm. Because the tubes are not developable, we cut out a flat sheet for each of the cross-section edges, and use tabs to adhere the multiple sheets together (figure 18*a*). This or a

similar methodology would need to be used for manufacturing the polygonal origami out of flat sheets. When extending origami to the medium scales it is possible to use layered composites where a flexible sheet that allows folding is sandwiched between more rigid panels [2,8,45]. Large origami structures could be constructed by using thickened panels interconnected by hinges rather than fold lines. For various applications in the real world the finite thickness of origami sheets begins to affect the system behaviour, and the idealized zero-thickness assumptions are no longer valid. Current research aims to account for thickness in kinematics and manufacturing in order to prevent self-intersection while minimizing the size of the stowed structure [30–32]. To make the reconfigurable polygonal tubes reliable and cost effective for industrial applications more innovation will still be needed. In particular, research should explore: materials and systems to allow multiple folding/unfolding cycles; rapid fabrication methods; mechanisms to facilitate deployment; and incorporating thickness into the tube design. The programmable switches of the polygonal tubes may also require new methods for rapid or remote actuation and reconfiguration.

## (c) Non-linear deformations and extensions

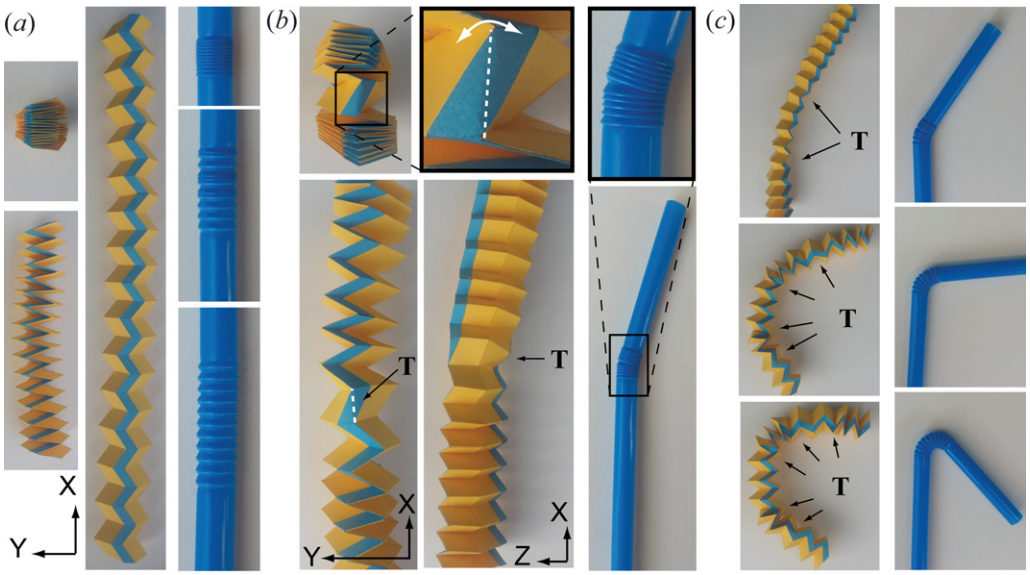


**Figure 19.** Localized distortion in the six-sided origami tube (left) can bring about new non-linear behaviours similar to those of bendable drinking straws (right). (*a*) Unfolding of the structures in the prescribed *straight* direction. (*b*) A single *transition* point indicated by a T is introduced in the origami tube. At this point a panel of the reconfigurable segment bends across its diagonal, allowing for a change in configuration to occur in the middle of the tube. (*c*) Multiple transition points lead to a global curvature over the length of the tube.

Most research on origami, as well as the body of this paper, take advantage of only the rigid and prescribed folding mechanisms of the system. However, some recent findings have shown that there exists a wide range of origami deformations where bending in the panels is encouraged [12,46]. These deformations could be substantially more complex than the rigid kinematics, and could correspond to highly non-linear behaviours of the thin sheet origami. In figure 19*b* we show localized bending that occurs on one of the switch panels of a polygonal tube with six edges. This allows the tube to have different cross-section configurations at different locations of the tube, i.e. Configuration I: below the transition point T and Configuration II: above it. The tube is initially constructed straight with 30 constant angle projections, but with the transition point there is a shift in the direction that the tube follows. Although each transition points causes a localized change

in direction, as more transition points are included, the origami tube can go from a straight to a curved structure. This phenomena is similar to conventional bending drinking straws 19*c*. The physical models of the polygonal tubes also showed some bistable and multi-stable effects, similar to other origami structures [46–48]. Multi-stability with the reconfigurable tubes could provide new ideas and applications. More complex tube cross-sections where more switches could be augmented, or longer tubes could lead to other interesting bending and non-linear effects.

## References


1. Randall CL, Gultepe E, Gracias DH. 2012 Self-folding devices and materials for biomedical applications. *Trends Biotechnology* **30**, 138-46.
2. Ma KY, Felton SM, Wood RJ. 2012 Design, fabrication, and modelling of the split actuator microrobotic bee. *IEEE/RSJ Int. Conf. on Intelligent Robots and Systems* (Vilamoura, Portugal) pp. 1133-1140.
3. Greenberg HC, Gong ML, Magleby SP, Howell LL. 2011 Identifying links between origami and compliant mechanisms. *Mech. Sci.* **2**, 217-225.
4. Martinez RV, Fish CR, Chen X, Whitesides GM. 2012 Elastomeric origami: Programmable paper-elastomer composites as pneumatic actuators. *Advanced Functional Mater.* **22**, 1376-1384.
5. Lang RJ. 2011 *Origami Design Secrets*, 2nd edn. CRC Press.
6. Barbarino S, Bilgen O, Ajaj RM, Friswell MI, Inman DJ. 2011 A review of morphing aircraft. *J. Intelligent Mater. Systems and Struct.* **22**, 823-877.
7. Del Grosso AE, Basso P. 2010 Adaptive building skin structures. *Smart Mater. and Struct.* **19**, 124011.
8. Hawkes E, An B, Benbernoub NM, Tanaka H, Kim S, Demaine ED, Rus D, Wood RJ. 2010 Programmable matter by folding. *Proc. Natl. Acad. Sci. USA* **107**, 12441-12445.
9. Marras AE, Zhou L, Su H-J, Castro CE. 2015 Programmable motion of DNA origami mechanisms. *Proc. Natl. Acad. Sci. USA* **112**, 713-718.
10. Fuchi K, Diaz AR, Rothwell EJ, Ouedraogo RO, Tang J. An origami tunable metamaterial. *J. Appl. Phys.* **111**, 084905.
11. Schenk M, Guest SD. 2013 Geometry of Miura-folded metamaterials. *Proc. Natl. Acad. Sci. USA* **110**, 3276-3281.
12. Silverberg JL, Evans AA, McLeod L, Hayward RC, Hull T, Santangelo CD, Cohen I. 2014 Using origami design principles to fold reprogrammable mechanical metamaterials. *Science* **345**, 647-650.
13. Filipov ET, Tachi T, Paulino GH. 2015 Origami tubes assembled into stiff, yet reconfigurable structures and metamaterials. *Proc. Natl. Acad. Sci. USA* **112**, 12321-12326.
14. Kuribayashi K, Tsuchiya K, You Z, Tomus D, Umemoto M, Ito T, Sasaki M. 2006 Self-deployable origami stent grafts as a biomedical application of Ni-rich TiNi shape memory alloy foil. *Mater. Sci. and Eng. A* **419**, 131-137.
15. Schenk M, Kerr SG, Smyth AM, Guest SD. 2013 Inflatable cylinders for deployable space structures. *Proc. the First Conference Transformables 2013 in the Honor of Emilio Perez Piñero* Seville, Spain.
16. Schenk M, Viquerat AD, Seffen KA, Guest SD. 2014 Review of inflatable booms for deployable space structures: Packing and rigidization. *J. of Spacecraft and Rockets* **51**, 762-778.
17. Yasuda H, Yein T, Tachi T, Miura K, Taya M. 2013 Folding behaviour of Tachi-Miura polyhedron bellows. *Proc. R. Soc. A* **469**, 20130351.
18. Francis KC, Rupert LT, Lang RJ, Morgan DC, Magleby SP, Howell LL. 2014 From crease pattern to product: considerations to engineering origami-adapted designs. *Proc. ASME 2014 IEDTC & CIEC* (Buffalo, NY) pp. V05BT08A030.
19. Song J, Chen Y, Lu G. 2012 Axial crushing of thin-walled structures with origami patterns. *Thin-Walled Struct.* **54**, 65-71.
20. Ma J, You Z. 2013 Energy absorption of thin-walled square tubes with a prefolded origami pattern-Part I: Geometry and numerical simulation. *J. Appl. Mech.* **81**, 011003.

21. Ma J, You Z. 2013 Energy absorption of thin-walled beams with a pre-folded origami pattern. *Thin-Walled Struct.* **73**, 198-206.
22. Gattas JM, You Z. 2015 The behaviour of curved-crease foldcores under low-velocity impact loads. *Int. J. Solids. Struct.* **53**, 80-91.
23. Cheung KC, Tachi T, Calisch S, Miura K. 2014 Origami interleaved tube cellular materials. *Smart Mater. and Struct.* **23**, 094012.
24. Li S, Wang KW. 2015 Fluidic origami with embedded pressure dependent multi-stability: a plant inspired innovation. *J. R. Soc. Interface* **12**: 20150639.
25. Miura K, Tachi T. 2010 Synthesis of rigid-foldable cylindrical polyhedra. *J. the Int. Soc. for the Interdisciplinary Study of Symmetry* (Gmuend, Austria) pp. 204-313.
26. Yasuda H, Yang J. 2015 Reentrant origami-based metamaterials with negative poisson's ratio and bistability. *Phys. Rev. Lett.* **114**, 185502.
27. Tsunoda H, Senbokuya Y, and Watanabe M. 2005 Deployment characteristics evaluation of inflatable tubes with polygon folding under airplane microgravity environment. *Space Tech.* **25**, 127-137.
28. Tachi T. 2009 One-Dof cylindrical deployable structures with rigid quadrilateral panels. *Proc. Int. Assoc. Shell and Spatial Struct.* (Valencia, Spain) pp. 2295-2305.
29. Tachi T, Miura K. 2012 Rigid-foldable cylinders and cells. *J. Int. Assoc. Shell and Spatial Struct.* **53**, 217-226.
30. Hoberman C. 2010 Folding structures made of thick hinged sheets - US Patent #7,794,019 B2,14.
31. Tachi T. 2011 Rigid-foldable thick origami. *Origami 5*, eds Wang-Iverson P, Lang RJ, Yim M (CRC) pp. 253-263.
32. Chen Y, Peng R, You Z. 2015 Origami of thick panels. *Science* **349**, 396-400.
33. Filipov ET, Tachi T, Paulino GH. 2015 Toward optimization of stiffness and flexibility of rigid, flat-foldable origami structures. *Origami 6* (In press).
34. Huffman DA. 1976 Curvature and creases: A primer on paper. *IEEE Trans. Comput.* **C-25**, 1010-1019.
35. Hull TC. 2012 *Project origami: activities for exploring mathematics*, 2nd edn. CRC Press.
36. belcastro sm, Hull TC. 2002 Modelling the folding of paper into three dimensions using affine transformations. *Linear Algebra and its Applications* **348**, 273-282.
37. belcastro sm, Hull TC. 2002 A mathematical model for non-flat origami. *Origami 3* pp. 39-51.
38. Tachi T. 2009 Simulation of rigid origami. *Origami 4* pp. 175-187.
39. Tachi T, Filipov ET, Paulino GH 2015 Deployable folded-core sandwich panels guided by a generating surface. *Proc. Int. Assoc. Shell and Spatial Struct.* Amsterdam, Netherlands (Accepted).
40. Gattas JM, You Z. 2015 Geometric assembly of rigid-foldable morphing sandwich structures. *Engineering Structures* 94:149-159.
41. Abaqus FEA 2010 Version 6.10 Documentation, Dassault Systemes Simulia Corp. Providence, RI, USA.
42. Briassoulis D 1986 Equivalent orthotropic properties of corrugated sheets. *Comput. Struct.* **23**, 129-138.
43. Tachi T. 2009 Generalization of rigid foldable quadrilateral mesh origami. *Proc. Int. Assoc. Shell and Spatial Struct.* (Valencia, Spain) pp. 2287-2294.
44. Deng D, Chen Y. 2013 An origami inspired additive manufacturing process for building thin-shell structures. *ASME 2013 IMECE Volume 2A: Advanced Manufacturing* (San Diego, CA) pp. V02AT02A016.
45. Peraza-Hernandez EA, Hartl DJ, Malak Jr RJ, Lagoudas DC. 2014 Origami-inspired active structures: a synthesis and review. *Smart Mater. and Struct.* **23**, 094001.
46. Silverberg JL, Na J-H, Evans AA, Liu B, Hull TC, Santangelo CD, Lang RJ, Hayward RC, Cohen I. 2015 Origami structures with a critical transition to bistability arising from hidden degrees of freedom. *Nature Mater.* **14**, 389-393.
47. Hanna BH, Lund JM, Lang RJ, Magleby SP, Howell LL. 2014 Waterbomb base: a symmetric single-vertex bistable origami mechanism. *Smart Mater. and Struct.* **23**, 094009.

48. Waitukaitis S, Menaut R, Chen BG-g, van Hecke M. 2015 Origami Multistabilty: From Single Vertices to Metasheets. *Phys. Rev. Lett.* **114**, 055503.